Journal of Materials Chemistry A

Materials for energy and sustainability

www.rsc.org/MaterialsA

Volume 1 | Number 36 | 28 September 2013 | Pages 10555–11080

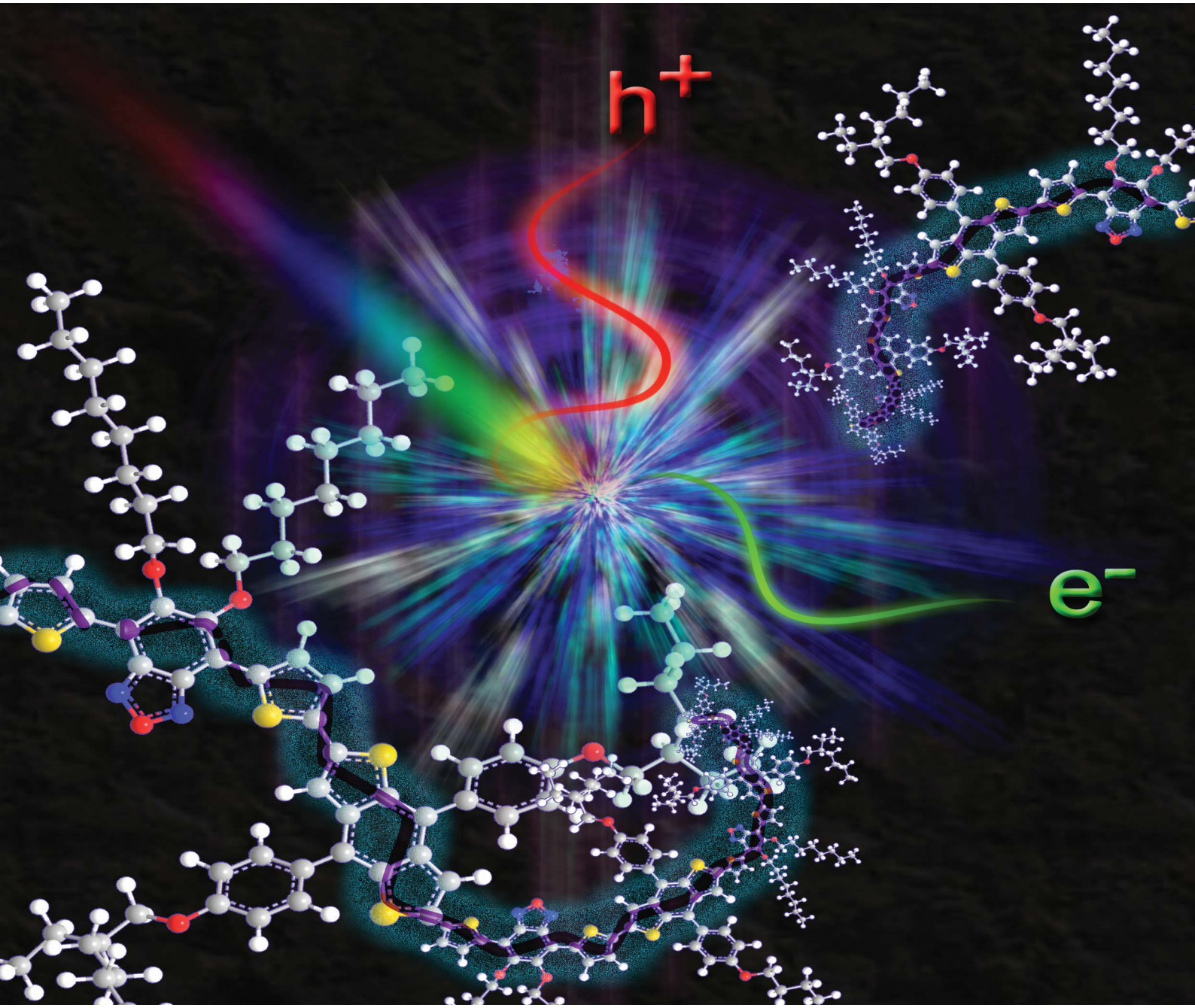

ISSN 2050-7488

RSC Publishing

PAPER

Yingping Zou *et al.*

New alkoxylphenyl substituted benzo[1,2-*b*:4,5-*b*′] dithiophene-based polymers: synthesis and application in solar cells

2050-7488(2013)1:36;1-S

Journal of Materials Chemistry A

RSC Publishing

PAPER

View Article Online
View Journal | View Issue

Cite this: J. Mater. Chem. A, 2013, 1, 10639

New alkoxylphenyl substituted benzo[1,2-*b*:4,5-*b*′] dithiophene-based polymers: synthesis and application in solar cells†

Jun Yuan,‡[a] Lu Xiao,‡[a] Bo Liu,‡[ab] Yongfang Li,[c] Yuehui He,[b] Chunyue Pan[a] and Yingping Zou*[ad]

Received 20th May 2013
Accepted 16th June 2013

DOI: 10.1039/c3ta11968h

www.rsc.org/MaterialsA

Two new alkoxylphenyl substituted benzo[1,2-*b*:4,5-*b*′]dithiophene (BDTPO)-based polymers (PBDTPO-DTBO and PBDTPO-DTBT) were synthesized. Their structures were verified by NMR spectroscopy, the molecular weights were determined by gel permeation chromatography (GPC), and the thermal properties were investigated by thermogravimetric analysis (TGA). UV-Vis absorption spectra of the polymers show broad and strong absorption bands from 300–750 nm both in $CHCl_3$ solutions and films. The resulting copolymers exhibit relatively deep HOMO energy levels (−5.56 and −5.46 eV) and surprisingly high hole mobilities (2.2×10^{-1} and 3.3×10^{-2} cm^2 V^{-1} s^{-1}) for PBDTPO-DTBO and PBDTPO-DTBT, respectively. Preliminary photovoltaic properties of the copolymers blended with [6,6]-phenyl-$C_{71\ (or\ 61)}$-butyric acid methyl ester (PCBM) as an electron acceptor were investigated. The polymer solar cell (PSC) based on the single layer device structure of ITO/PEDOT:PSS/PBDTPO-DTBO:$PC_{71}BM$ (1 : 1.5, w/w)/Ca/Al demonstrates a high power conversion efficiency of 6.2% under the illumination of AM 1.5G, 100 mW cm^{-2}.

Introduction

The past several years have witnessed tremendous progress in polymer solar cells (PSCs), due to their easy fabrication, simple device structure, light weight nature and capability to be used to fabricate flexible devices. Bulk heterojunction (BHJ) PSCs, which are based on the conjugated polymer donor (D) and the fullerene derivative acceptor (A), show a typical organic photovoltaic device structure.[1] The most classical studied photovoltaic device using soluble poly(3-hexlthiophene) (P3HT) as the donor and the fullerene derivative as the acceptor under the standard AM 1.5G, 100 mW cm^{-2} illumination can achieve a power conversion efficiency (PCE) up to 7.4%.[2,3] PCE is proportional to short circuit current density (J_{sc}), open-circuit voltage (V_{oc}) and fill factor (FF). Three main factors are responsible for the low PCE of PSCs. One is that the relatively large bandgap cannot harvest solar radiation efficiently, resulting in a low J_{sc}. Another is the low V_{oc} of PSCs resulting from the relatively high HOMO (highest occupied molecular orbital), because V_{oc} is generally related to the difference between the HOMO level of the donor and the LUMO (lowest unoccupied molecular orbital) level of the acceptor.[4] Finally, low and unbalanced mobilities also exert some effects on J_{sc} and FF. For developing higher PCE of PSCs, conjugated polymers with relatively broad absorption, suitable energy levels, good solubility in common organic solvents and high mobility are extraordinarily important.[5,6]

Presently, the copolymerization of donor unit and acceptor unit is a very effective way to construct ideal high efficiency polymers. Much effort has been devoted to the design and synthesis of new donor and acceptor building blocks.[7] To date, alkoxyl or alkylthienyl substituted benzodithiophene (BDT or BDTT) have proven to be excellent donor building blocks.[8]

Meanwhile, the advantages of BDT or BDT derivatives are: it is easy to synthesize, relatively easy modifications and planar conjugated structures which could be beneficial to the electron delocalization; furthermore, some BDT-based polymers also show high hole mobilities.[9] In this work, we choose two typical electron accepting units with alkoxyl groups: 4,7-di(5-bromothien-2-yl)-5,6-dioctyloxybenzo[*c*][1,2,5]oxadiazole (**M1**)[8,10–12] and 4,7-di(5-bromothien-2-yl)-5,6-dioctyloxy benzo[*c*] [1,2,5]oxadiazole (**M2**).[8,10–12] Our group have reported the copolymerization

[a]College of Chemistry and Chemical Engineering, Central South University, Changsha 410083, China. E-mail: yingpingzou@csu.edu.cn

[b]State key Laboratory for Powder Metallurgy, Central South University, Changsha 410083, China

[c]Beijing National Laboratory for Molecular Sciences, Institute of Chemistry, Chinese Academy of Sciences, Beijing 100190, China

[d]Key Laboratory of Resources Chemistry of Nonferrous Metals (Central South University), Ministry of Education, Changsha, Hunan 410083, China

† Electronic supplementary information (ESI) available: ^1H NMR spectra of the monomer, UV-visible absorption spectra, *J*–*V* curves, EQEs of devices are shown in the Fig. S1–S6, respectively. Optical and electrochemical data are summarized in Table S1, photovoltaic data are summarized in Tables S2 and S3. See DOI: 10.1039/c3ta11968h

‡ J. Yuan, L. Xiao and B. Liu contributed equally to this work.

of **M1** or **M2** with alkylthienyl substituted benzodithiophene (BDTT) unit, these kinds of polymers exhibit broad absorption, suitable energy levels and good photovoltaic properties with a PCE reaching 5.9%.[13] Very recently, Yang and coworkers have reported two alkylphenyl substituted benzodithiophene (BDTP) based copolymers using diketopyrrolopyrrole (DPP) derivatives as the electron accepting units, without any device modification, two polymers show a very low PCE of 0.5–2%, furthermore, when using 1% 1,8-diiodooctane (DIO) as the solvent additive, the PCE of PBDTP-DPP surprisingly increased up to 6% from 1.5% and the polymers were applied in tandem solar cells, PCE close to *ca.* 9% was reached.[14] However, the stability of the polymers and the PCEs for commercial solar cells is not high enough, thus it is still necessary for us to do further explorations of new D–A conjugated polymers for photovoltaic applications.

Replacing the alkyl chain using alkoxyl group can increase the electron donating ability and enhance the coplanarity.[15] Herein, we designed and synthesized two new copolymers namely PBDTPO-DTBO and PBDTPO-DTBT, which the alkoxylphenyl substituted BDT, namely BDTPO, was used as the electron donor unit with **M1** and **M2** as electron accepting units. The relationship between the structure and properties has been investigated in detail. The copolymers showed good solubility in common organic solvents and broad absorption from 300–750 nm. In addition, the blend films suggested hole mobilities up to 2.2×10^{-1} cm^2 V^{-1} s^{-1} and 3.3×10^{-2} cm^2 V^{-1} s^{-1} respectively for PBDTPO-DTBO and PBDTPO-DTBT, measured by the SCLC method. The PSCs based on PBDTPO-DTBO as donor and $PC_{71}BM$ as acceptor demonstrated a PCE up to 6.2% with a V_{oc} of 0.89 V, a J_{sc} of 11 mA cm^{-2} and FF of 64%, under the illumination of AM1.5, 100 mW cm^{-2}.

Experimental section

Materials

4-Bromophenol, *n*-BuLi, $Pd(PPh_3)_4$, tetrahydrofuran (THF) and $Sn(CH_3)_3Cl$ were obtained from Aladdin and Alfa Asia Chemical Co., and they were used without further purification. Toluene was dried over molecular sieves and freshly distilled prior to use. Other reagents and solvents were purchased commercially as ACS-grade quality and used without further purification. Compound **3**,[13] **M1** (ref. 8 and 12) and **M2** (ref. 8 and 12) were synthesized according to the reported literature. All the other compounds were synthesized following the procedures described herein.

Characterization

^1H NMR spectra were recorded using a Bruker AV-400 spectrometer in deuterated chloroform solution at 298 K, unless specified otherwise. Chemical shifts were reported as δ values (ppm) with tetramethylsilane (TMS) as the internal reference. Mass spectroscopy was carried out using an Agilent mass spectrometer. Elemental analysis was performed on a Flash EA 1112 elemental analyzer. Molecular weights and polydispersities of the polymers were determined by gel permeation chromatography (GPC) analysis with polystyrene as the standard (Waters 515 HPLC pump), a Waters 2414 differential refractometer, and three Waters Styragel columns (HT2, HT3 and HT4) using THF (HPLC grade) as eluent at a flow rate of 1.0 mL min^{-1} at 35 °C. Thermogravimetric analysis (TGA) was conducted on a Perkin-Elmer TGA-7 with a heating rate of 20 K min^{-1} under nitrogen. UV-Vis absorption spectra were recorded on the SHIMADZU UV-2450 spectrophotometer. For the solid state measurements, polymer solution in chloroform was spin-coated on quartz plates. The cyclic voltammetry was recorded with a computer controlled Zahner IM6e electrochemical workstation using polymer films on platinum electrode (1.0 cm^2) as the working electrode, a platinum wire as the counter electrode and Ag/AgCl (0.1 M) as the reference electrode in an anhydrous and argon-saturated solution of 0.1 M of tetrabutylammonium hexafluorophosphate (Bu_4NPF_6) in acetonitrile at a scanning rate of 50 mV s^{-1}. Electrochemical onsets were determined at the position where the current starts to differ from the baseline. The morphologies of the polymer/$PC_{71}BM$ blend films were investigated by a SPI 3800N atomic force microscope (AFM) in contacting mode with a 5 μm scanner.

Fabrication and characterization of polymer solar cells

The PSCs were fabricated in the configuration of the traditional sandwich structure with an indium tin oxide (ITO) glass anode and a Ca/Al cathode. Patterned ITO glass with a sheet resistance of 15–20 Ω/□ was purchased from CSG HOLDING Co. Ltd (China). The ITO glass was cleaned by sequential ultrasonic treatment in detergent, deionized water, acetone and isopropanol, and then treated in an ultraviolet-ozone chamber (Ultraviolet Ozone Cleaner, Jelight Company, USA) for 25 min. Then PEDOT:PSS (poly(3,4-ethylene dioxythiophene):poly(styrene sulfonate)) (Baytron PVP Al 4083, Germany) was filtered through a 0.45 μm poly(tetrafluoroethylene) (PTFE) filter and spin coated at 2000 rpm for 40 s on the ITO substrate. Subsequently, PEDOT:PSS film was baked at 150 °C for 15 min in the air, and the thickness of the PEDOT:PSS layer is about 40 nm. The polymers and $PC_{71}BM$ (10 mg mL^{-1} for polymers) were dissolved in *ortho*-dichlorobenzene (*o*-DCB) overnight and spin-cast at 2000 rpm for 45 s onto the PEDOT:PSS layer. The thickness of the photoactive layer is about 150 nm measured by Ambios Technology XP-2 profilometer. A bilayer cathode consisting of Ca (~20 nm) capping with Al (~80 nm) was thermal evaporated under a shadow mask with a base pressure of *ca.* 10^{-5} Pa. The active area of the PSCs is 4 mm^2. Device characterization was carried out under AM 1.5G irradiation with the intensity of 100 mW cm^{-2} (Oriel 67005, 500 W), calibrating by a standard silicon cell. *J–V* curves were recorded with a Keithley 236 digital source meter. A xenon lamp with AM1.5 filter was used as the white light source and the optical power was 100 mW cm^{-2}. The EQE measurements of PSCs were performed by Stanford Systems model SR830 DSP lock-in amplifier coupled with a WDG3 monochromator and 500 W xenon lamp. A calibrated silicon detector was used to determine the absolute photosensitivity at different wavelengths. All of the fabrication and characterization after cleaning of ITO substrates was conducted in a glove box.

Synthesis of the monomers and polymers

The synthetic routes for the monomer and copolymers are shown in Scheme 1. The detailed synthetic processes for the compounds and polymers are as follows.

1-Bromo-4-(2′-ethylhexyloxy)benzene (2)

4-Bromophenol (**1**) (8.6 g, 50 mmol), K_2CO_3 (8.3 g, 60 mmol) were put into a three-neck round-bottom flask, and then 200 mL DMF was added. Under the argon atmosphere, 1-bromo-2-ethylhexane (9.5 g, 50 mmol) was added dropwise *via* a syringe. The mixture was heated to 150 °C overnight in the dark. And then cooled to room temperature and the reaction mixture was poured into 200 mL water and then extracted three times with chloroform. The organic extraction was washed successively with saturated potassium hydroxide and water for twice, respectively. The combined organic phases were dried over magnesium sulfate. After filtration, the solvents were evaporated under vacuum and the crude product was purified on a silica gel column eluting with petroleum ether. Brown oil was obtained (10.3 g, 73% yield). ^{1}H NMR (400 MHz, $CDCl_3$, ppm): δ: 7.36 (d, 2H); 6.80 (d, 2H); 3.97 (d, 2H); 1.79 (m, 1H); 154–1.36 (m, 8H); 0.96 (s, 6H). MS: $m/z = 284$ (M^+).

4,8-Bis(4-ethylhexyloxy-1-phenyl)-benzo[1,2-*b*:4,5-*b*′]-dithiophene (4)

Under vigorous stirring, 1-bromo-4-(2-ethylhexyloxy)benzene (7.87 g, 27.6 mmol) was added dropwise to magnesium turnings (0.797 g, 33.2 mmol) in anhydrous THF (35 mL) which was protected by argon. During the process, I_2 (10 mg) was added as a catalyst for the reaction. The solution was refluxed for 5 h until the magnesium was consumed. The mixture was refluxed for one more hour and then was cooled down. The solution system was added slowly to benzo[1,2-*b*:4,5-*b*′]dithiophene-4,8-dione (2.03 g, 9.22 mmol) dispersed in 40 mL THF. $SnCl_2$ (13.3 g) was dissolved in 10% aqueous HCl (18.6 mL) and then added dropwise into the above reaction mixture. The solution was stirred for another 1 h at 50 °C. After cooling to room temperature, the mixture was poured into water and extracted with dichloromethane, the organic extraction was washed successively with water and sodium bicarbonate solution twice and the combined organic phase was dried over magnesium sulfate and evaporated to afford the crude product. The crude product was purified on a silica gel column, eluting with pure hexane. White crystals were obtained (1.7 g, 31% yield).^{1}H NMR (400 MHz, $CDCl_3$, ppm): δ: 7.63 (d, 4H), 7.36 (m, 4H), 7.09 (d, 4H), 3.95 (d, 4H), 1.80 (m, 2H), 1.56–1.38 (br, 16H), 0.97 (m, 12H). MS: $m/z = 598$ (M^+).

2,6-Bis(trimethyltin)-4,8-bis(4-ethylhexyloxy-1-phenyl)-benzo[1,2-*b*:4,5-*b*′]-dithiophene (M3)

A solution of compound **4** (0.9 g 1.5 mmol) in dry THF (30 mL) was deoxygenated with nitrogen for 30 min, and then 2.4 M *n*-butyllithium solution in *n*-hexane (1.8 mL, 4.32 mmol) was added dropwise at 0 °C. Then the solution was allowed to warm up to 50 °C for 1 h, and 1.0 M trimethyltin chloride solution in THF (10 mL, 10 mmol) was added. Then the mixture was poured into water and extracted with dichloromethane. The organic phase was evaporated, and the residue was recrystallized from 20 mL acetone to afford the pale yellow solid (0.75 g, 55%). ^{1}H NMR (400 MHz, $CDCl_3$, ppm): δ: 7.65 (d, 4H), 7.38 (s, 2H), 7.11 (d, 4H), 3.96 (d, 4H), 1.80 (m, 2H), 1.58 (br, 16H), 0.97 (m, 12H), 0.35 (t, 18H). MS: $m/z = 924$ (M^+).

Synthesis of PBDTPO-DTBO

M1 (0.14 g, 0.2 mmol), **M3** (0.185 g, 0.2 mmol) and 12 mL of dry toluene were put into a two-necked flask. The solution was flushed with Ar for 20 min, then $Pd(PPh_3)_4$ (15 mg) was added into the flask. The solution was flushed with Ar again for 20 min. The oil bath was heated to 110 °C carefully, and the reactant was stirred for 24 h at this temperature under argon atmosphere. Then the reaction mixture was cooled to room temperature and then poured into methanol (100 mL) slowly. The resulting precipitate was filtered through a Soxhlet thimble, which was then subjected to Soxhlet extractions with methanol, hexane and chloroform. Finally the polymer was recovered as a solid from the chloroform fraction by rotary evaporation. Finally, the black-blue solid was obtained (0.08 g, yield: 35%). ^{1}H NMR (400 MHz, $CDCl_3$, ppm): δ: 7.71–7.63 (br, 8H), 7.16–7.10 (br, 6H), 4.30–4.00 (br, 8H), 1.82–1.70 (m, 2H), 1.54–0.89 (br, 58H). Anal. calcd for $(C_{68}H_{82}N_2O_5S4)n$ (%): C, 71.93; H, 7.28; N, 2.47. Found (%): C, 71.24; H, 7.35; N, 2.56.

Synthesis of PBDTPO-DTBT

PBDTPO-DTBT was obtained by the similar procedure with the synthesis of PBDTPO-DTBO starting from **M2** (0.071 g, 0.1 mmol) and **M3** (0.091 g, 0.1 mmol). Finally, the black-blue solid was obtained (0.077 g, yield: 66%). ^{1}H NMR (400 MHz, $CDCl_3$,

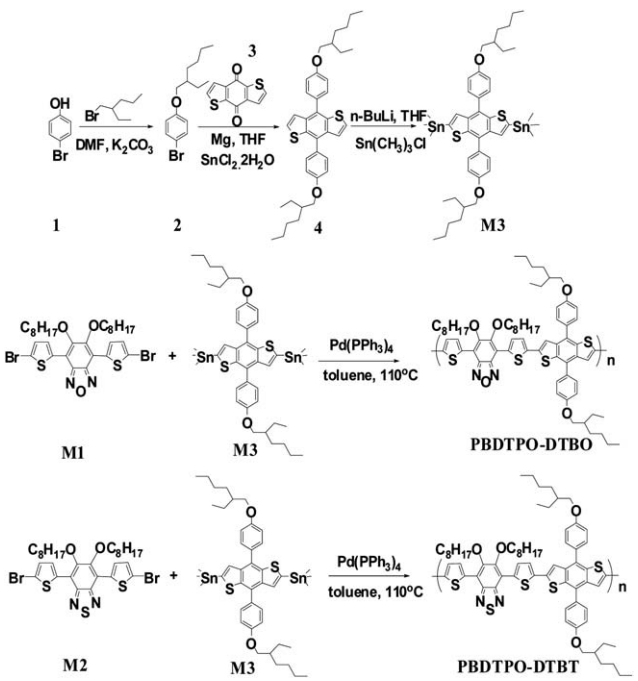

Scheme 1 Synthetic routes for the monomer and the corresponding polymers.

ppm): δ: 7.76–7.48 (br, 8H), 7.15–6.99 (br, 6H), 4.13–4.00 (br, 8H), 1.91–1.86 (m, 2H), 1.52–0.87 (br, 58H). Anal. calcd for $(C_{68}H_{82}N_2O_4S_5)n$ (%):C, 70.93; H, 7.18; N, 2.43. Found (%): C, 70.56; H, 7.05; N, 2.48.

Results and discussion

Material synthesis

The general synthetic routes for the monomer and polymers are shown in Scheme 1. The new monomer **M3** was synthesized *via* a Grignard reaction as shown in Scheme 1 and the ^{1}H NMR spectroscopy of the monomer **M3** is shown in Fig. S1. 1-Bromo-4-(2′-ethylhexyloxy)benzene was treated with magnesium in tetrahydrofuran (THF) under argon to form the Grignard reagent, and then the reagent was transferred to another flask containing benzodithiophenedione dispersed in THF under argon. The nucleophilic reaction completed upon heating to 50 °C for 1 h. After reduction by $SnCl_2$, 4,8-bis(4-ethylhexyloxy-1-phenyl)-benzo[1,2-*b*:4,5-*b*′]-dithiophene (**4**) was obtained as a white crystal. **M3** was copolymerized with the dibromide derivatives (**M1** and **M2**) through Stille coupling reactions to obtain the target polymers PBDTPO-DTBO and PBDTPO-DTBT, respectively. The polymers were purified by continuous Soxhlet extractions with methanol, hexane and $CHCl_3$. And then the $CHCl_3$ fraction was concentrated under vacuum evaporation, precipitated into methanol and collected by filtration, to yield a black-blue solid. The molecular weights of the polymers were determined by gel-permeation chromatography (GPC) using THF as eluent and polystyrene as the standard. The number average molecular weights (M_n) of PBDTPO-DTBO, PBDTPO-DTBT are 17 kDa and 18 kDa, with a PDI of 1.6 and 1.4, respectively, the related data are summarized in Table 1. Both polymers exhibit good solubility in common organic solvents such as chloroform, toluene and *o*-dichlorobenzene (*o*-DCB).

Thermal stability

The thermogravimetric curves (TGA) are depicted in Fig. 1. PBDTPO-DTBO and PBDTPO-DTBT exhibit good thermal stability, with 5% weight-loss temperatures (T_d) at 309 °C and 316 °C under an inert atmosphere, respectively. The polymerization results and thermal data for the polymers are shown in Table 1. The thermal curves of the two copolymers are similar, which indicates that both polymers' thermal stability is adequate for application in optoelectronic devices.

Optical properties

The absorption spectra of the polymers in $CHCl_3$ solutions and solid films are shown in Fig. 2, the combined absorption from the solutions and films are included in Fig. S2, and the related data are summarized in Table S1.† PBDTPO-DTBO and PBDTPO-DTBT films display broad absorption spectra. Both polymers show two absorption bands in the wavelength range of 350–750 nm, the peaks in the long wavelength region locate at 567 nm and 633 nm, the peaks in the short wavelength region lie at 422 nm and 432 nm, respectively for PBDTPO-DTBO and PBDTPO-DTBT. Compared to the solutions, two polymers are more red-shifted and have broader absorption in the film states, indicating that the planar structure of BDTPO is capable of inducing strong π–π interactions. Compared to PBDTPO-DTBT, PBDTPO-DTBO's UV-Vis absorption has a red-shift in solution

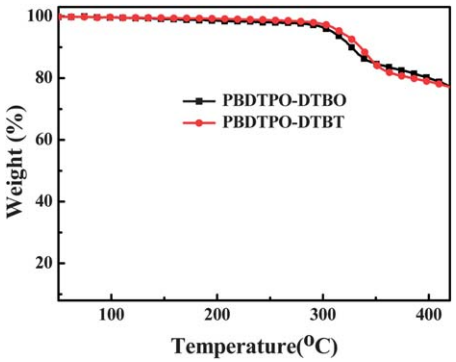

Fig. 1 TGA curves of the polymers with a heating rate of 20 K min^{-1}.

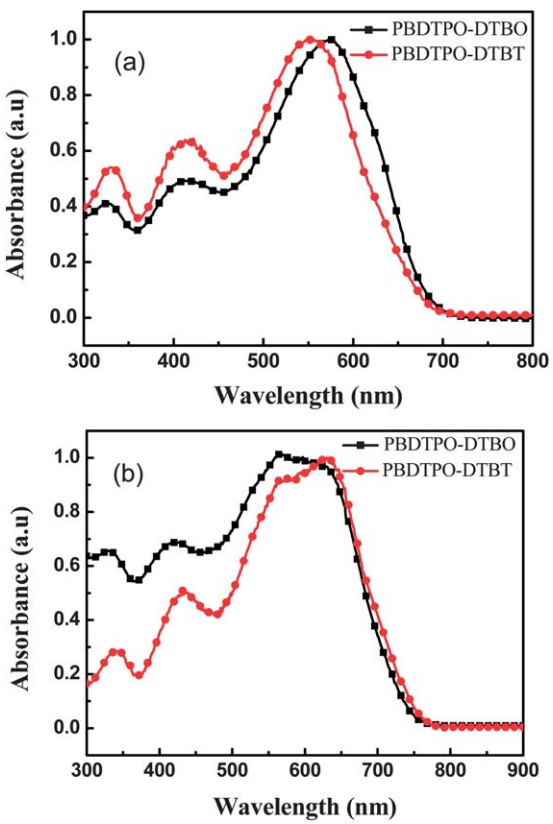

Fig. 2 UV-Vis absorption spectra of PBDTPO-DTBO and PBDTPO-DTBT: (a) solutions in dilute $CHCl_3$ and (b) films on quartz cast from $CHCl_3$ solution.

Table 1 Molecular weights and thermal properties of the copolymers

Polymers	M_n (kDa)	M_w (kDa)	PDI	Yield (%)	T_d (°C)
PBDTPO-DTBO	17	26.5	1.6	35	309
PBDTPO-DTBT	18	24.3	1.4	66	316

and a blue-shift in film, which may be due to the stronger interaction in the PBDTPO-DTBT solid film. From the onset of the thin film absorptions, we can estimate the optical bandgaps of 1.65 eV and 1.62 eV for PBDTPO-DTBO and PBDTPO-DTBT, respectively. Compared with their alkylthienyl substituted BDT based copolymer,[13,16] BDTPO based polymers show slightly lower bandgap, which is originated from the extended conjugation by replacing alkylthienyl group with alkoxylphenyl unit.

Electrochemical properties

The electrochemical properties of the two copolymers were investigated by cyclic voltammetry (CV). As shown in Fig. 3, the oxidation onset potentials of PBDTPO-DTBO and PBDTPO-DTBT are 1.16 V and 1.06 V, respectively. The reduction onset potentials of PBDTPO-DTBO and PBDTPO-DTBT are −0.72 V and −0.74 V, respectively. The highest occupied molecular orbital (HOMO) and lowest occupied molecular orbital (LUMO) energy levels of the polymers can be calculated according to the following equations: HOMO = −e (E_{ox} + 4.4) (eV) and LUMO = −e (E_{red} + 4.4) (eV), where the unit of E_{ox} and E_{red} are in V *vs.* Ag/AgCl. The HOMO and LUMO levels of PBDTPO-DTBO and BDTPO-DTBT are −5.56 eV/−3.68 eV and −5.46 eV/−3.66 eV, respectively. From the typical CV curves, the energy levels of the copolymers can be tuned by altering the electron with-drawing units. PBDTPO-DTBO has the deeper HOMO level due to higher electronegativity of oxygen atom from DTBO unit compared to sulfur atom from DTBT unit (O, 3.5; S, 2.5), which ensured good air stability and a high V_{oc} in the PSCs.[9,14] The relatively deeper HOMO energy levels (−5.4 to −5.6 eV) could be expected to afford higher V_{oc} in PSC applications, which is one of main contributors to obtain high efficiency polymer solar cells. The electrochemical bandgaps, estimated from the difference between the HOMO and LUMO energy levels, were 1.88 eV and 1.80 eV for PBDTPO-DTBO and PBDTPO-DTBT respectively. The electrochemical bandgaps are slightly larger than the optical bandgaps. This discrepancy might have been induced by the presence of an energy barrier at the interface between the polymer film and the electrode surface.[17] The optical and electronic energy level data of the polymers were also listed in Table S1.†

Hole mobility

Charge mobility is another important parameter for conjugated polymers, because of its direct effect on charge transport. Hole-only devices (ITO/PEDOT:PSS/polymer/Au) were fabricated in order to estimate the hole mobilities of these polymers *via* space-charge limit current (SCLC) theory.[18] We measured the hole mobilities of PBDTPO-DTBO, and PBDTPO-DTBT blended with $PC_{71}BM$ by the SCLC method based on the Poole–Frenkel law which is described as

$$J_{SCLC} = \frac{9}{8}\varepsilon_0\varepsilon_r\mu_0\frac{(V-V_{bi})^2}{d^3}\exp\left[0.89\gamma\sqrt{\frac{V-V_{bi}}{d}}\right] \quad (1)$$

where J is the current density, μ_0 is the zero-field mobility, ε_0 is the dielectric permittivity of the vacuum, ε_r is relative dielectric permittivity of the material, d stands for the thickness of the device, and $V = V_{appl} - V_{bi}$, where V_{appl} is the applied potential and V_{bi} is the built-in potential. The results are plotted as $\ln(Jd^3/V^2)$ *vs.* $(V/d)^{0.5}$, as shown in Fig. 4. According to eqn (1) and Fig. 4, the hole mobilities of PBDTPO-DTBO and PBDTPO-DTBT are calculated to be 2.2×10^{-1} and 3.3×10^{-2} $cm^2\ V^{-1}\ s^{-1}$, respectively. We can see that the hole mobility of the PBDTPO-DTBO blend was higher than that of PBDTPO-DTBT blend under the same conditions. PBDTPO-DTBO has exhibited a comparable hole mobility compared to that of BDTT based polymer (PBDTT-DTBO with a mobility of 4.9×10^{-1} $cm^2\ V^{-1}\ s^{-1}$),[13] originating from the good planarity of BDTPO.

Photovoltaic properties

To explore and compare the photovoltaic performance of PBDTPO-DTBO and PBDTPO-DTBT, BHJ PSC devices were fabricated with a single layer configuration of ITO/PEDOT:PSS/polymer:PCBM/Ca/Al. Fig. 5(a) shows the typical *J*–*V* curves of the PSC under the illumination of AM 1.5, 100 mW cm^{-2}. The corresponding V_{oc}, J_{sc}, FF and PCE of the devices are summarized in Table 2. Different weight ratios of polymer donor to $PC_{61}BM$ (1 : 1 and 1 : 2) were investigated, which were used to optimize the device performance, the detailed device results have been summarized in Table S2 and Fig. S3.† The best device

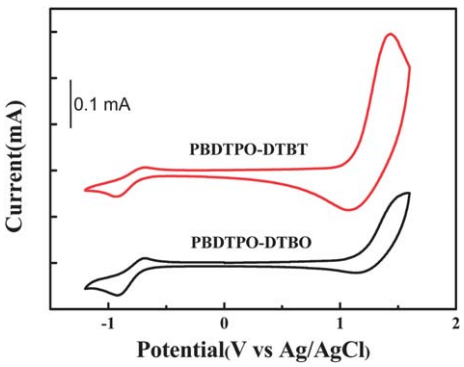

Fig. 3 Cyclic voltammograms of PBDTPO-DTBO and PBDTPO-DTBT films on a platinum electrode in 0.1 M Bu_4NPF_6, CH_3CN solution.

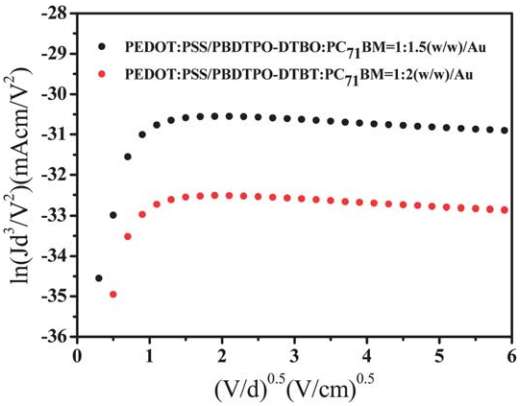

Fig. 4 Ln (Jd^3/V^2) *vs.* $(V/d)^{0.5}$ plots of the blends of PBDTPO-DTBO, PBDTPO-DTBT and $PC_{71}BM$ for measurement of the hole mobilities by the SCLC method.

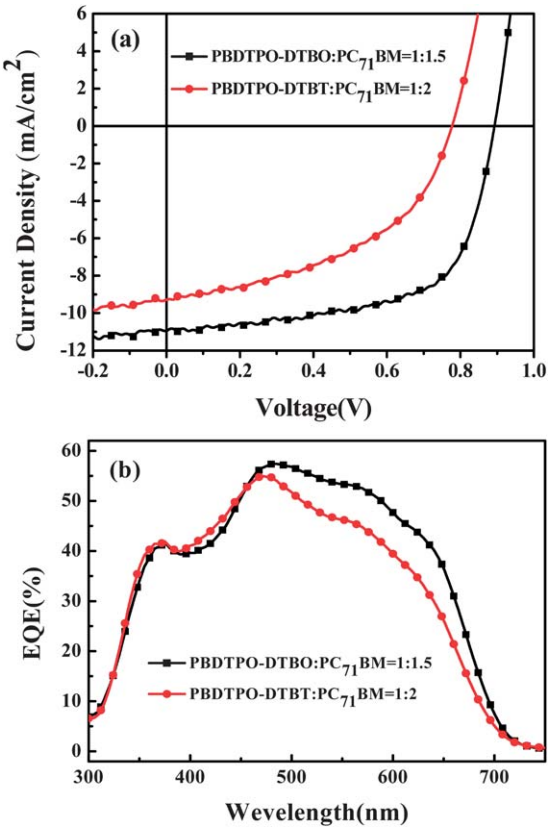

Fig. 5 (a) Typical *J*–*V* curves of the PSCs based on PBDTPO-DTBO and PBDTPO-DTBT : $PC_{71}BM$ (1 : 1.5 and 1 : 2, w/w), under illumination of AM 1.5, 100 mW cm^{-2}. (b) EQE spectra of PSCs based on PBDTPO-DTBO and PBDTPO-DTBT:$PC_{71}BM$ (1 : 1.5 and 1 : 2, w/w).

performance was achieved with donor (D)/acceptor (A) weight ratio of the PBDTPO-DTBO:$PC_{61}BM$ of 1 : 2, w/w, reaching 5.0% with V_{oc} = 0.89 V, J_{sc} = 8.7 mA cm^{-2} and FF = 64%. When the D/A weight ratio of PBDTPO-DTBO and $PC_{61}BM$ decreases to 1 : 1, the PCE reduces to 3.2%. For the PBDTPO-DTBT:$PC_{61}BM$ blend at 1 : 1 weight ratio, the device reaches the highest device efficiency up to 2.6%. The large decrease of the PCE of PBDTPO-DTBT compared to PBDTPO-DTBO is mainly originated from the reduction of J_{sc} and V_{oc}. Instead of $PC_{61}BM$, $PC_{71}BM$ was chosen as the acceptor material due to the stronger light-harvesting ability in the visible region with a broad absorption from 440 to 530 nm, which possesses complementary absorption to that of the polymers.[19] When the copolymers are blended with $PC_{71}BM$, the weight ratio of PBDTPO-DTBO : $PC_{71}BM$ was optimized to be 1 : 1.5 to obtain the best device performance and exhibited a PCE of 6.2% with a V_{oc} of 0.89 V, a J_{sc} of 11 mA cm^{-2} and a FF of 64%. Among the two polymers, PBDTPO-DTBO shows the better photovoltaic properties because of the higher J_{sc} and V_{oc}. The detailed photovoltaic properties are shown in Fig. S3 and S4† and the related photovoltaic data are summarized in Tables S2 and S3† The relatively deep-lying HOMO resulted in the higher V_{oc}, and the J_{sc} of the device is strongly dependent on the bandgap and mobility of the conjugated polymer.[20] As investigated above, PBDTPO-DTBO has a comparable bandgap and higher hole mobility, which allows for a higher J_{sc} in the device compared to PBDTPO-DTBT. Moreover higher hole mobility of PBDTPO-DTBO also resulted in relatively higher FF. Moreover, deep HOMO level has led to high V_{oc} up to 0.9 V of PBDTPO-DTBO. The first two BDTPO based polymers' results indicated that BDTPO (alkoxylphenyl substituted BDT) is a promising new donor building block for constructing D–A copolymers in PSCs.

Table 2 Photovoltaic performances of the polymer solar cells based on PBDTPO-DTBO and PBDTPO-DTBT

Active layer	V_{oc} (V)	J_{sc} (mA cm^{-2})	FF (%)	PCE (%)
PBDTPO-DTBO:$PC_{71}BM$ = 1 : 1.5	0.89	11	64	6.2
PBDTPO-DTBT:$PC_{71}BM$ = 1 : 2	0.78	9.3	47	3.4

The external quantum efficiency (EQE) of the BHJ device was measured to verify the accuracy of the above devices, and the typical EQE curves are shown in Fig. 5(b). All the devices showed a high incident PCE with a broad response from 300 nm to 700 nm, and the maximum EQE plateau reached 50% from 445–600 nm. From the photovoltaic measurements, the EQE for the PBDTPO-DTBT based devices decreases slightly compared with that of PBDTPO-DTBO. This also agrees well with the result of a relatively lower J_{sc} observed for the PBDTPO-DTBT based devices.

Morphology

To understand the photovoltaic properties of the resulting polymers, we investigated the morphologies of blends with the two different D/A ratios spin-coated from their *o*-dichlorobenzene solution by tapping-mode atomic-force microscope (AFM). The height and phase images of the blend films are shown in Fig. 6(A and B). The surface of PBDTPO-DTBO:$PC_{71}BM$ (1 : 1.5, w/w) and PBDTPO-DTBT:$PC_{71}BM$ (1 : 2, w/w) films are relatively uniform with the root-mean-square (RMS) roughness of 2.01 and 1.33 nm,

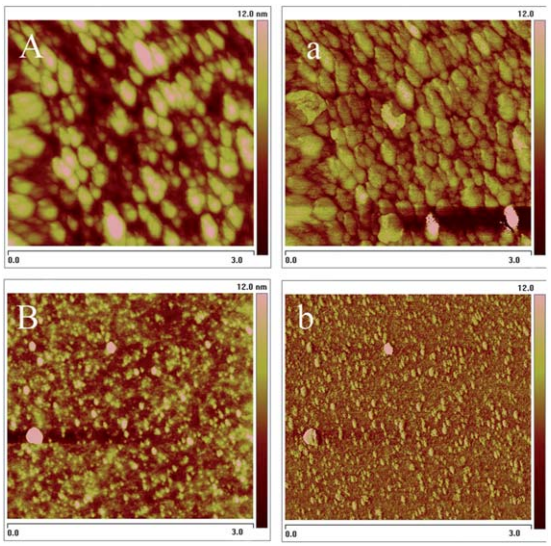

Fig. 6 AFM height images (A and B) and phase images (a and b) of the blend films of PBDTPO-DTBO/$PC_{71}BM$ (1 : 1.5, w/w) and PBDTPO-DTBT/$PC_{71}BM$ (1 : 2, w/w) prepared by spinning-coating with *o*-dichlorobenzene solution.

respectively. From the phase images Fig. 6(a and b), the PBDTPO-DTBO/$PC_{71}BM$ blend film show some aggregation and nano-phase separation, which to some extent explains the higher photovoltaic properties of PBDTPO-DTBO/$PC_{71}BM$.[21]

Conclusions

In summary, a new BDT derivative-BDTPO was firstly synthesized. Two new low bandgap BDTPO based conjugated polymers (PBDTPO-DTBO and PBDTPO-DTBT) were designed, synthesized and applied in PSCs. Copolymers showed good solubility in common organic solvents, broad visible absorption from 300 to 750 nm, deep HOMO level (−5.4 to −5.6 eV) and surprisingly high hole mobilities (10^{-1} and 10^{-2} cm^2 V^{-1} s^{-1}). The single-layer photovoltaic device from the PBDTPO-DTBO/$PC_{71}BM$ (1 : 1.5, w/w) blend showed a high PCE, up to 6.2% with $V_{oc} = 0.89$ V, $J_{sc} = 11$ mA cm^{-2}, FF = 64%. These results clearly indicated that BDTPO is a new and promising electron donor unit for constructing high efficiency photovoltaic materials.

Acknowledgements

We thank Xuewen Chen for the data analysis. This work was supported by NSFC (no. 51173206, 21161160443), National High Technology Research and Development Program (no. 2011AA050523) and China Postdoctoral Science Foundation.

Notes and references

1 Y. Li, *Acc. Chem. Res.*, 2012, **45**, 723.
2 M. R. Reyes, K. Kim and D. L. Carroll, *Appl. Phys. Lett.*, 2005, **87**, 083506.
3 G. Li, V. Shrotriya, J. Huang, Y. Yao and Y. Yang, *Nat. Mater.*, 2005, **4**, 864.
4 B. C. Thompson and J. M. J. Frechet, *Angew. Chem., Int. Ed.*, 2008, **47**, 58.
5 Y. Li and Y. Zou, *Adv. Mater.*, 2008, **20**, 2952.
6 Z. Gu, P. Shen, S. Tsang, Y. Tao, B. Zhao, P. Tang, Y. Nie, Y. Fang and S. Tan, *Chem. Commun.*, 2011, **47**, 9381.
7 Y. Yang, J. H. Hou, H. Y. Chen, S. Q. Zhang and G. Li, *J. Am. Chem. Soc.*, 2008, **130**, 16144.
8 P. Ding, C. Zhong, Y. Zou, C. Pan, H. Wu and Y. Cao, *J. Phys. Chem. C*, 2011, **115**, 16211.
9 B. Liu, X. Chen, Y. Zou, L. Xiao, X. Xu, Y. He, L. Li and Y. Li, *Macromolecules*, 2012, **45**, 6898.
10 P. Ding, C. Chu, B. Liu, B. Peng, Y. Zou, Y. He, K. Zhou and C. Hsu, *Macromol. Chem. Phys.*, 2010, **211**, 2555.
11 Z. Zhang, B. Peng, B. Liu, C. Pan, Y. Li, Y. He, K. Zhou and Y. Zou, *Polym. Chem.*, 2010, **1**, 1441.
12 J. Bouffard and T. M. Swager, *Macromolecules*, 2008, **41**, 5559.
13 B. Liu, X. Chen, Y. He, Y. Li, X. Xu, L. Xiao, L. Li and Y. Zou, *J. Mater. Chem.*, 2013, **1**, 570.
14 L. Dou, J. Gao, E. Richard, J. You, C. Chen, K. C. Cha, Y. He, G. Li and Y. Yang, *J. Am. Chem. Soc.*, 2012, **134**, 10071.
15 R. Qin, W. Li, C. Li, C. Du, C. Veit, H. F. Schleiermacher, M. Andersson, Z. Bo, Z. Liu, O. Inganäs, U. Wuerfel and F. Zhang, *J. Am. Chem. Soc.*, 2009, **131**, 14612.
16 Q. Peng, X. Liu, D. Su, G. Fu, J. Xu and L. Dai, *Adv. Mater.*, 2011, **23**, 4554.
17 Y. Li, Y. Cao, J. Gao, D. Wang, G. Yu and A. J. Heeger, *Synth. Met.*, 1999, **99**, 243.
18 C. Chen, Y. Cheng, C. Chang and C. Hsu, *Macromolecules*, 2011, **44**, 8415.
19 (*a*) Y. Yao, C. Shi, G. Li, V. Shrotriya, Q. Pei and Y. Yang, *Appl. Phys. Lett.*, 2006, **89**, 153507; (*b*) Z. Gu, P. Shen, S. Tsang, Y. Tao, B. Zhao, P. Tang, Y. Nie, Y. Fang and S. Tan, *Chem. Commun.*, 2011, **47**, 9381.
20 (*a*) K. Vandewal, K. Tvingstedt, A. Gadisa, O. Inganas and J. V. Manca, *Nat. Mater.*, 2009, **8**, 904; (*b*) M. D. Perez, C. Borek, S. R. Forrest and M. E. Thompson, *J. Am. Chem. Soc.*, 2009, **131**, 9281; (*c*) A. Najari, S. Beaupre, P. Berrouard, Y. Zou, J. Pouliot, C. Lepage and M. Leclerc, *Adv. Funct. Mater.*, 2011, **21**, 718.
21 W. Li, Y. Zhou, B. V. Andersson, L. M. Andersson, Y. Thomann, C. Veit, K. Tvingstedt, R. Qin, Z. Bo, O. Inganas, U. Würfel and F. Zhang, *Org. Electron.*, 2011, **12**, 1544.